Universität des Saarlandes

Fachrichtung 6.1 – Mathematik

Preprint Nr. 297

Higher order BEM-based FEM on polygonal meshes

Sergej Rjasanow and Steffen Weißer

Saarbrücken 2011

Fachrichtung 6.1 – Mathematik
Universität des Saarlandes

Preprint No. 297
submitted: September 27, 2011

Higher order BEM-based FEM on polygonal meshes

Sergej Rjasanow

Saarland University
Department of Mathematics
P.O. Box 15 11 50
66041 Saarbrücken
Germany
rjasanow@num.uni-sb.de

Steffen Weißer

Saarland University
Department of Mathematics
P.O. Box 15 11 50
66041 Saarbrücken
Germany
weisser@num.uni-sb.de

Edited by
FR 6.1 – Mathematik
Universität des Saarlandes
Postfach 15 11 50
66041 Saarbrücken
Germany

Fax: + 49 681 302 4443
e-Mail: preprint@math.uni-sb.de
WWW: http://www.math.uni-sb.de/

Higher order BEM-based FEM on polygonal meshes

Sergej Rjasanow Steffen Weißer

September 27, 2011

Abstract

The BEM-based finite element method is reviewed and extended with higher order basis functions on general polygonal meshes. These functions are defined implicitly as local solutions of the underlying homogeneous problem with constant coefficients. They are treated by means of boundary integral formulations and are approximated using the boundary element method in the numerics. To obtain higher order convergence, a new approximation of the material coefficient is proposed since previous strategies are not sufficient. Following recent ideas, error estimates are proven which guarantee quadratic convergence in the H^1-norm. The numerical realization is discussed and several experiments confirm the theoretical results.

1 Introduction

In the field of numerical methods for partial differential equations there is an increasing interest for non-simplicial meshes. Several applications in solid mechanics, biomechanics as well as geological science show the need for general elements within a finite element simulation. Discontinuous Galerkin methods [6] and mimetic finite difference methods [2] are able to handle such kind of meshes. Nevertheless, these two strategies yield nonconforming approximations which are not in the Sobolev-space in which the exact solution lies.

Already in 1975, Wachspress [18] proposed the construction of conforming rational basis functions on convex polygons with any number of sides. In recent years, several improved basis functions on polygonal elements have been introduced and applied in linear elasticity [16] or computer graphics [10], for example. There are even the first attempts which seek to introduce quadratic finite elements on polygons [13].

In [4], a new kind of conforming finite element method on polygonal meshes has been proposed which uses basis functions that fulfil the differential equation locally. In the local problems constant material parameters and vanishing right

hand side are prescribed. In case of the diffusion equation harmonic basis functions are recovered. This method has been studied in several articles concerning convergence [9] and residual error estimates for adaptive mesh refinement [19]. In the following, the theory is extended to a higher order method on polygonal meshes.
The outline of this article is as follows. In Section 2, some notation as well as a model problem are introduced. We review the first order method proposed in [4] and give a definition for regular meshes. The BEM-based FEM is extended to a higher oder scheme in Section 3. Afterwards, we introduce interpolation operators in Section 4 and prove interpolation properties which yield error estimates for the finite element method on polygonal meshes in the $H^1(\Omega)$-norm. In Section 5, a new approximation of the diffusion coefficient is proposed since existing strategies are not sufficient for higher order. Finally, we discuss the numerical realisation in Section 6.

2 Starting point and preliminaries

Let $\Omega \subset \mathbb{R}^2$ be a bounded polygonal domain with Lipschitz boundary $\Gamma = \overline{\Gamma}_D \cup \overline{\Gamma}_N$ and $|\Gamma_D| > 0$. For given data $f \in L_2(\Omega)$, $g_D \in H^{1/2}(\Gamma_D)$ and $g_N \in L_2(\Gamma_N)$, the boundary value problem we are dealing with reads

$$\begin{aligned} -\mathrm{div}(a(x)\nabla u(x)) &= f(x) \quad \text{for } x \in \Omega, \\ u(x) &= g_D(x) \quad \text{for } x \in \Gamma_D, \\ a(x)\nabla u(x) \cdot n(x) &= g_N(x) \quad \text{for } x \in \Gamma_N, \end{aligned}$$

where $n(x)$ denotes the outer normal vector of Ω at x and $a \in L_\infty(\overline{\Omega})$ is a scalar function with

$$0 < a_{\min} \leq a(x) \leq a_{\max} \quad \text{for } x \in \overline{\Omega}.$$

Since $g_D \in H^{1/2}(\Gamma_D)$, an extension u_D of g_D exists with $u_D \in H^1(\Omega)$. A natural way to find the solution $u \in H^1(\Omega)$ of the problem is to use the representation $u = u_D + u_0$ with $u_0 \in V$, where

$$V = H^1_D(\Omega) = \{v \in H^1(\Omega) : \gamma_0 v = 0 \text{ on } \Gamma_D\}$$

with the trace operator $\gamma_0 : H^1(\Omega) \to H^{1/2}(\Gamma)$ defined in [1]. Due to this decomposition, we obtain the variational formulation

$$\text{Find } u_0 \in V : \quad a_\Omega(u_0, v) = (f, v) + (g_N, v)_{\Gamma_N} - a_\Omega(u_D, v), \quad \forall v \in V$$

with the L_2-scalar products $(\cdot,\cdot)$ and $(\cdot,\cdot)_{\Gamma_N}$ over Ω and Γ_N, respectively, and the bilinear form

$$a_\Omega(u, v) = \int_\Omega a(x)\nabla u(x) \cdot \nabla v(x)\, dx.$$

The properties of a ensure that $a_\Omega(\cdot,\cdot)$ is coercive and bounded on V. Therefore, the problem has a unique solution according to the Lax-Milgram theorem.
For the finite element method, we have to introduce a discretization $\mathcal{K}_h$ of Ω. In contrast to classical methods, we allow meshes with arbitrary convex polygonal elements which are bounded. The elements $K \in \mathcal{K}_h$ are open sets which are non-overlapping such that

$$\overline{\Omega} = \bigcup_{K \in \mathcal{K}_h} \overline{K}.$$

Here, the closure of a set K is denoted by $\overline{K}$. The elements consist of nodes and edges. An edge E is always located between two nodes, the start and the end point, which are also the only nodes on E. In each corner of an element K, a node is located but there could also be some nodes on straight lines of the boundary ∂K. This behaviour is natural to polygonal meshes and improves the approximation properties of the finite element solution. In triangular or quadrilateral meshes such nodes appear as hanging nodes which are undesirable and do not influence the accuracy of the approximation.
The length of an edge E and the diameter of an element K are denoted by h_E and $h_K = \sup\{|x-y| : x, y \in \partial K\}$, respectively. We introduce the diameter ρ_K of the largest circle inscribed in K with center z_K. If z_K is not unique an arbitrary but fixed one is chosen.

Definition 1. The mesh $\mathcal{K}_h$ is called regular if it fulfils:

1. The aspect ratio is uniformly bounded from above by σ, i.e. $h_K/\rho_K < \sigma \quad \forall K \in \mathcal{K}_h$.

2. All elements $K \in \mathcal{K}_h$ are convex polygons.

Additionally, we assume that $h_K < 1$ for all elements $K \in \mathcal{K}_h$. This condition is no grievous restriction on the mesh, since $h_K < 1$ can always be satisfied by scaling Ω. Nevertheless, it is necessary in the forthcoming local boundary integral formulations.

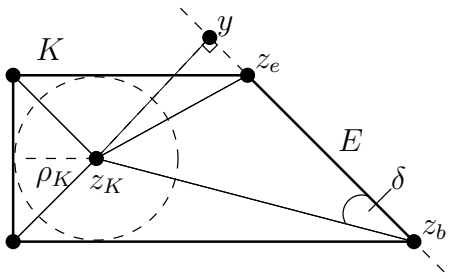

Figure 1: Element K with inscribed circle, auxiliary triangulation and projection y of z_K onto the straight line through E

Remark 1. This definition of a regular mesh is different from the one proposed in [19]. Instead of the assumption on the aspect ratio there are two other criteria

- There is a constant $c_1 > 0$ such that for all elements $K \in \mathcal{K}_h$ and all its edges $E \subset \partial K$ we have $h_K \leq c_1 h_E$.
- There is an angle α_0 with $0 < \alpha_0 \leq \pi/3$ such that for all elements $K \in \mathcal{K}_h$ and all its edges $E \subset \partial K$ the isosceles triangle with longest side E and two interior angles α_0 lies inside the element K.

The first one is an additional assumption and the second one follows from the criterion on the aspect ratio. This can be seen as follows. We construct a triangulation of $K \in \mathcal{K}_h$ by connecting all vertices $z \in \partial K$ with z_K. Next we bound the angles between the new introduced edges and the previous ones $E = \overline{z_b z_e} \subset \partial K$ from below, see 1. Without loss of generality, we assume that the angle δ is smaller than $\pi/2$. Using the projection y of z_K onto the straight line through the edge E we can recognize

$$\sin \delta = \frac{|y - z_K|}{|z_b - z_K|} \geq \frac{\rho_K}{h_K} \geq \frac{1}{\sigma}.$$

Consequently, it is $\delta \geq \arcsin \sigma^{-1}$. Since this estimate is valid for all angles next to ∂K of the auxiliary triangulation, the isosceles triangles prescribed in [19] with $\alpha_0 = \min\{\pi/3, \arcsin \sigma^{-1}\}$ lie inside the auxiliary triangles and therefore inside K.

Let $\mathcal{K}_h$ be a regular mesh and $\mathcal{N}_h = \mathcal{N}_{h,\Omega} \cup \mathcal{N}_{h,D} \cup \mathcal{N}_{h,N}$ the set of nodes in the mesh, where $\mathcal{N}_{h,\Omega}$, $\mathcal{N}_{h,D}$ and $\mathcal{N}_{h,N}$ contain the nodes of the interior of Ω, on the Dirichlet boundary Γ_D and in the interior of the Neumann boundary Γ_N, respectively. The transition points between Γ_D and Γ_N belong to $\mathcal{N}_{h,D}$.
Next, we review the lowest order nodal trial functions which are used in [4, 19], for example. For every $z \in \mathcal{N}_h$, the function ψ_z is defined as unique solution of

$$\begin{gathered} -\Delta \psi_z = 0 \quad \text{in } K \quad \text{for all } K \in \mathcal{K}_h, \\ \psi_z(x) = \begin{cases} 1 & \text{for } x = z \\ 0 & \text{for } x \in \mathcal{N}_h \setminus \{z\} \end{cases}, \\ \psi_z \text{ is linear on each edge of the mesh.} \end{gathered}$$

Therefore, the trial functions ψ_z are defined as solutions of local boundary value problems (in K) and it is well known that ψ_z is arbitrary smooth in the interior of K and continuous on the closure of K for $K \in \mathcal{K}_h$, see [7]. Let

$$\Psi^{(1)} = \{\psi_z : z \in \mathcal{N}_h\} \quad \text{and} \quad \Psi_D = \{\psi_z : z \in \mathcal{N}_{h,D}\}.$$

To obtain a discrete Galerkin-formulation, we introduce the space

$$V_h = \operatorname{span} \Psi \quad \text{with} \quad \Psi = \Psi^{(1)} \setminus \Psi_D$$

which is conforming in the sense $V_h \subset V$ as well as a discrete extension u_{Dh} of the Dirichlet boundary data. For simplicity, we choose the interpolation of g_D with trial functions $\psi_z \in \Psi_D$ as extension of u_{Dh}. The Galerkin-formulation reads

$$\text{Find } u_{0h} \in V_h : \quad a_\Omega(u_{0h}, v_h) = (f, v_h) + (g_N, v_h)_{\Gamma_N} - a_\Omega(u_{Dh}, v_h), \quad \forall v_h \in V_h$$

and yields a system of linear equations for the ansatz

$$u_{0h} = \sum_{\psi \in \Psi} \beta_\psi \psi \quad \text{and} \quad v_h \in \Psi. \tag{1}$$

The approximation of the unknown function u is finally given by $u_h = u_{0h} + u_{Dh}$. The drawback of this formulation is that one has to integrate the gradient of the implicitly defined trial functions over the interior of the elements. Under the restriction that the material coefficient $a(\cdot)$ is constant on each element $K \in \mathcal{K}_h$ it is possible to rewrite the formulation. In [4], a variational problem has been found which is only formulated on the so called skeleton of the mesh. All involved integrals were reduced to the boundary of the elements where the trial functions are known explicitly.
The finite element method on polygonal meshes with lowest order harmonic trial functions yields linear convergence in the H^1-norm as well as quadratic convergence in the L_2-norm. This behaviour has been observed in [19].

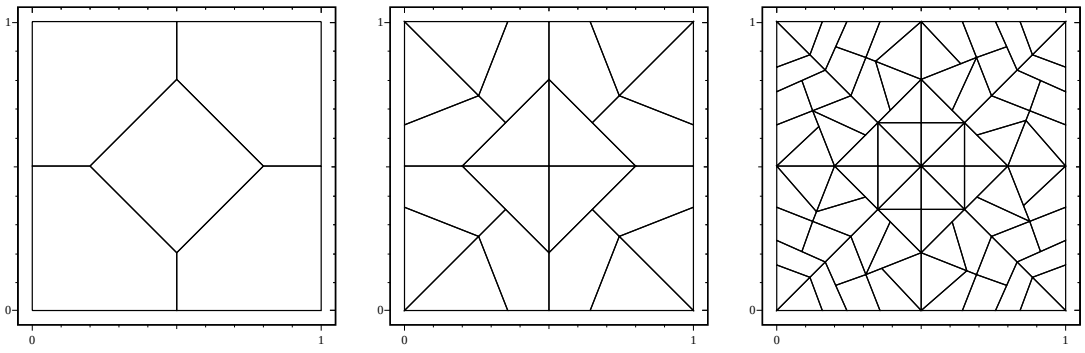

Figure 2: Initial mesh (left), refined mesh after two steps (middle), refined mesh after four steps (right)

Example 1. The function $u(x) = \exp(2\pi(x_1 - 0.3)) \cos(2\pi(x_2 - 0.3))$, $x \in \mathbb{R}^2$ fulfils

$$\begin{aligned} -\Delta u &= 0 \quad \text{in } \Omega = [0,1]^2, \\ u &= g_D \quad \text{on } \Gamma \end{aligned}$$

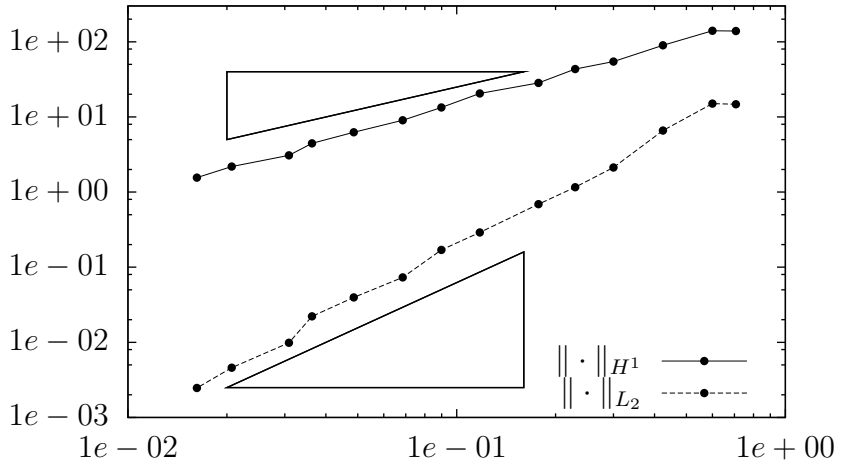

Figure 3: Absolute error with respect to h for Example 1 and triangles with slope one and two

with $g_D = \gamma_0 u$. The error is analysed with respect to $h = \max\{h_K : K \in \mathcal{K}_h\}$. The convergence can be seen in Figure 3 for the finite element method on a sequence of uniform refined meshes, compare Figure 2.

3 Extensions to higher order

The lowest order harmonic trial functions are understood quite well in uniform [8] and adaptive [19] strategies. Therefore, the question for higher order approximations arises. A straight forward generalization is to add harmonic trial functions which have quadratic boundary data.
The set of all edges of the mesh is denoted by $\mathcal{E}_h = \mathcal{E}_{h,\Omega} \cup \mathcal{E}_{h,D} \cup \mathcal{E}_{h,N}$, where $\mathcal{E}_{h,\Omega}$, $\mathcal{E}_{h,D}$ and $\mathcal{E}_{h,N}$ contain all edges in the interior of Ω, on the Dirichlet boundary Γ_D and the Neumann boundary Γ_N, respectively. We define for each edge $E \in \mathcal{E}_h$ a function ψ_E. Let $z_b, z_e \in \mathcal{N}_h$ be the nodes at the beginning and at the end of the edge $E = \overline{z_b z_e}$. Then, ψ_E is the unique solution of

$$\begin{aligned} -\Delta\psi_E &= 0 && \text{in } K \quad \text{for all } K \in \mathcal{K}_h, \\ \psi_E &= 4\,\psi_{z_b}\psi_{z_e} && \text{on } \widetilde{E} \quad \text{for all } \widetilde{E} \in \mathcal{E}_h. \end{aligned}$$

Due to the definition of ψ_E, it vanish on all edges of the mesh apart from E. The restriction of ψ_E onto E is the well known quadratic bubble function which is zero in the corner points and one at the midpoint of the edge. For $E \in \mathcal{E}_{h,\Omega}$, we have $\operatorname{supp}\psi_E = \overline{K_1 \cup K_2}$ where $K_1, K_2 \in \mathcal{K}_h$ are the neighbouring elements of E with $E \subset \partial K_1 \cap \partial K_2$. If $E \in \mathcal{E}_{h,D} \cup \mathcal{E}_{h,N}$ belongs to the boundary of the domain Ω it has just one neighbouring element of course. Since the trial function

is harmonic in the interior of each element, ψ_E is arbitrary smooth in K and continuous on the closure of K for all $K \in \mathcal{K}_h$, see e.g. [7].
To obtain higher order convergence, we enrich the trial space $V_h = \operatorname{span} \Psi$ by adding the edge trial functions ψ_E to the basis Ψ. Therefore, we set

$$\Psi = \Psi^{(2)} \setminus \Psi_D$$

with

$$\Psi^{(2)} = \Psi^{(1)} \cup \{\psi_E : E \in \mathcal{E}_h\},$$

where we also have to enrich Ψ_D to

$$\Psi_D = \{\psi_z, \psi_E : z \in \mathcal{N}_{h,D}, E \in \mathcal{E}_{h,D}\}.$$

The discrete space V_h is now equipped with harmonic functions of higher polynomial order over the edges of the mesh. This space seems to suit to approximate harmonic functions with higher order. Consequently, we can use the enriched V_h in the Galerkin-formulation which was stated in Section 2. The boundary data g_D is now approximated by piecewise quadratic polynomials over Γ_D and the extension u_{Dh} is chosen as linear combination of trial functions $\psi \in \Psi_D$.

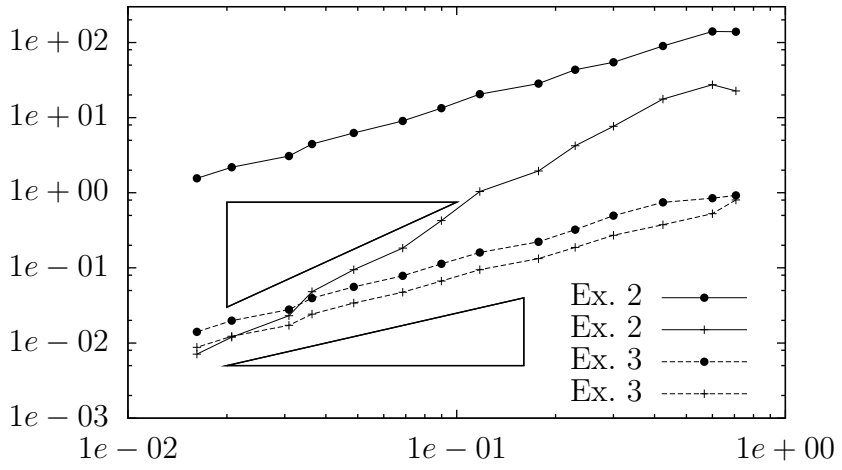

Figure 4: Absolute error in H^1-norm with respect to h for Example 2 and Example 3 with $\Psi = \Psi^{(1)} \setminus \Psi_D$ ($\bullet$) and $\Psi = \Psi^{(2)} \setminus \Psi_D$ ($+$), respectively, and triangles with slope two and one

Example 2. We solve again the Laplace problem mentioned in Example 1 for the harmonic function $u(x) = \exp(2\pi(x_1 - 0.3)) \cos(2\pi(x_2 - 0.3))$ and plot the convergence in Figure 4.

Example 3. Consider the Dirichlet boundary value problem

$$\begin{aligned} -\Delta u &= f \quad \text{in } \Omega = [0,1]^2, \\ u &= 0 \quad \text{on } \Gamma, \end{aligned}$$

where $f \in L_2(\Omega)$ is chosen in such a way that $u(x) = \sin(\pi x_1)\sin(\pi x_2)$ for $x \in \Omega$ is the exact solution. The convergence results can be found in Figure 4.

In the last two examples, we have seen that the trial space V_h fits quite well for problems with vanishing right hand side f but lacks in the general case. This behaviour is not surprising since an approximation $u_h \in V_h$ always satisfy $-\Delta u_h = 0$ in all $K \in \mathcal{K}_h$. It is necessary to enrich the trial space V_h even further. For each element $K \in \mathcal{K}_h$, we introduce a so called element bubble function ψ_K which fulfils

$$\begin{aligned} -\Delta \psi_K &= 1 \quad \text{in } K, \\ \psi_K &= 0 \quad \text{else} \end{aligned}$$

and is therefore uniquely defined. This function ψ_K is arbitrary smooth in K and continuous on the closure of K, see [7]. Adding these bubble functions to the basis

$$\Psi = \Psi^{(3)} \setminus \Psi_D$$

with

$$\Psi^{(3)} = \Psi^{(2)} \cup \{\psi_K : K \in \mathcal{K}_h\},$$

we obtain an improved trial space which is still conforming, i.e. $V_h = \operatorname{span} \Psi \subset V$. Using this final space V_h in the Galerkin-formulation to solve the Poisson problem in Example 3 we get the desired rates of convergence.

Example 4. We solve again the problem mentioned in Example 3 for the function $u(x) = \sin(\pi x_1)\sin(\pi x_2)$ and plot the convergence in Figure 5. Due to the enriched trial space, we get quadratic convergence in the energy norm and cubic convergence in the L_2-norm.

4 Interpolation estimate and FEM convergence

The common way to find convergence estimates for finite element methods is to use Céa's-Lemma and replace the minimum therein by an interpolation. If we have an appropriate interpolation operator $\mathfrak{I} : H^2(\Omega) \to V_h$ we get

$$\|u - u_h\|_{H^1(\Omega)} \leq c \min_{v_h \in V_h} \|u - v_h\|_{H^1(\Omega)} \leq c \|u - \mathfrak{I}u\|_{H^1(\Omega)}.$$

Obviously, the problem to find convergence estimates for finite element methods reduces to find a good interpolation operator and to study its properties.
In the following, we introduce three interpolation operators. The first one interpolates a given function $u \in H^2(\Omega)$ using lower order trial functions. This

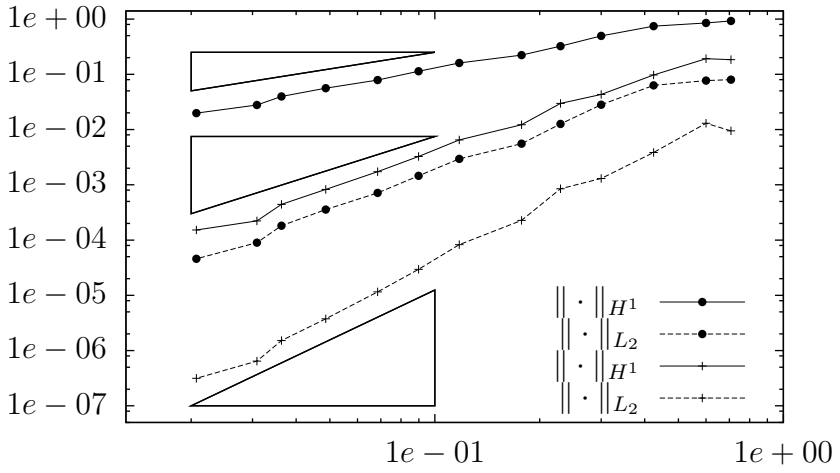

Figure 5: Absolute error with respect to h for Example 4 with $\Psi = \Psi^{(1)} \setminus \Psi_D$ ($\bullet$) and $\Psi = \Psi^{(3)} \setminus \Psi_D$ ($+$), respectively, and triangles with slope one, two and three

operator has already been studied in [8] and some interpolation estimates have been found. Additionally, we introduce two higher order interpolation operator and proof with similar but extended ideas new estimates. For $v \in H^2(\Omega)$, we define the operators $\mathfrak{I}^{(i)} : H^2(\Omega) \to H^1(\Omega)$, $i = 1, 2, 3$ as follows

$$\mathfrak{I}^{(i)} v = \sum_{\psi \in \Psi^{(i)}} \alpha_\psi \psi, \quad i = 1, 2, 3,$$

where

$$\alpha_{\psi_z} = v(z) \quad \text{for } z \in \mathcal{N}_h,$$

$$\alpha_{\psi_E} = v\left(\frac{z_b + z_e}{2}\right) - \left(\mathfrak{I}^{(1)} v\right)\left(\frac{z_b + z_e}{2}\right) \quad \text{for } E \in \mathcal{E}_h \text{ with } E = \overline{z_b z_e}$$

and

$$\alpha_{\psi_K} = \frac{1}{\psi_K(z_K)} \left(v(z_K) - \left(\mathfrak{I}^{(2)} v\right)(z_K)\right) \quad \text{for } K \in \mathcal{K}_h.$$

These operators use pointwise interpolation. Evaluations of functions $v \in H^2(\Omega)$ in one point are well defined because of the fact that $H^2(\Omega) \subset C^0(\Omega)$ in two dimensions according to the Sobolev embedding theorem.
Since we can decompose the $H^1(\Omega)$-norm into a sum of $H^1(K)$-norms over elements, it is enough to examine the interpolation properties over a single element. Let $\mathcal{P}^k(K)$ denote the space of polynomials over K with degree k.

Lemma 1. *The restrictions of the interpolation operators $\mathfrak{I}^{(i)}$, $i = 1, 2, 3$ to each element $K \in \mathcal{K}_h$ fulfil*

1. *$\mathfrak{I}^{(1)} p = p$ for $p \in \mathcal{P}^1(K)$,*

2. $\mathfrak{I}^{(2)}p = p$ *for* $p \in \mathcal{P}^2(K)$ *with* $\Delta p = 0$ *and*

3. $\mathfrak{I}^{(3)}p = p$ *for* $p \in \mathcal{P}^2(K)$,

Proof. Let $p \in \mathcal{P}^k(K)$ with $\Delta p = 0$ for $k = 1, 2$. Obviously, the trace of p on the boundary of K is a polynomial of degree k. Therefore, we can express this trace exactly with the trial functions out of $\Psi^{(k)}$ restricted to ∂K. It is

$$p\big|_{\partial K} = \mathfrak{I}^{(k)}p\big|_{\partial K} \tag{2}$$

and both p as well as $\mathfrak{I}^{(k)}p$ fulfil the Dirichlet problem

$$\begin{aligned} \Delta u &= 0 \quad \text{in } K, \\ u &= p \quad \text{on } \partial K. \end{aligned}$$

Since this problem has a unique solution, it follows that $\mathfrak{I}^{(k)}p = p$.
Next, we show $\mathcal{P}^2(K) \subset \operatorname{span} \Psi^{(3)}$. Let $p \in \mathcal{P}^2(K)$. As before, we can express the trace of p like in (2). Furthermore, we set $\alpha = \Delta p \in \mathbb{R}$ and

$$\widetilde{p} = \alpha\psi_K + \mathfrak{I}^{(2)}p \in \operatorname{span} \Psi^{(3)}. \tag{3}$$

Both functions p and $\widetilde{p}$ fulfil the boundary value problem

$$\begin{aligned} \Delta u &= \alpha \quad \text{in } K, \\ u &= p \quad \text{on } \partial K. \end{aligned}$$

Therefore, they are equal, i.e. $p = \widetilde{p}$. Solving (3) for α yields

$$\alpha = \frac{1}{\psi_K(x)} \left(p(x) - \mathfrak{I}^{(2)}p(x)\right) \quad \text{for } x \in K$$

which means $\alpha = \alpha_{\psi_K}$ and proves $\mathfrak{I}^{(3)}p = p$. □

Another property of the interpolation operator is the continuity. This has been shown for $\mathfrak{I}^{(1)}$ in [8]. In the subsequent lemma, we prove the corresponding estimate for the interpolation operator $\mathfrak{I}^{(3)}$ in a similar way. Lets assume that the diameter h_K of the element $K \in \mathcal{K}_h$ is one. This can be ensured by scaling. In the following, c denotes a generic constant that only depends on the maximal aspect ratio σ of the mesh given in Definition 1.

Lemma 2. *Let* $K \in \mathcal{K}_h$ *with* $h_K = 1$. *There exist a constant* $c = c(\sigma)$ *independent of* K *such that*

$$\|\mathfrak{I}^{(1)}v\|_{H^1(K)} \leq c\,\|v\|_{H^2(K)} \quad \textit{for } v \in H^2(K)$$

and

$$\|\mathfrak{I}^{(3)}v\|_{H^1(K)} \leq c\,\|v\|_{H^2(K)} \quad \textit{for } v \in H^2(K).$$

Proof. In this proof, we make use of the minimum-maximum principle which can be found in [7]. First, the second inequality is proven. Let $v \in H^2(K)$. The interpolation $\mathfrak{I}^{(3)}v$ fulfils the Dirichlet problem

$$\begin{aligned} \Delta\widetilde{v} &= \alpha_K \quad \text{in } K, \\ \widetilde{v} &= g_v \quad \text{on } \partial K \end{aligned} \tag{4}$$

in the classical sense with a piecewise quadratic function $g_v = \mathfrak{I}^{(3)}v\big|_{\partial K}$ on the boundary. Consequently, it also satisfies the weak formulation

$$\text{Find } \widetilde{v} \in H^1(K): \quad \gamma_0^K\widetilde{v} = g_v \quad \text{and} \quad \int_K \nabla\widetilde{v}\cdot\nabla w = (\alpha_K, w)_{L_2(K)}, \quad \forall w \in H_0^1(K).$$

To obtain homogeneous boundary data, we write $\widetilde{v} = \widetilde{v}_0 + \widetilde{v}_g$ where $\widetilde{v}_0 \in H_0^1(K)$ and $\widetilde{v}_g \in H^1(K)$ with $\widetilde{v}_g = g_v$. According to Proposition 5 in [8], the triangulation of K which is obtained by connecting $z_K \in K$ with all vertices of K is regular with respect to a constant $C = C(\sigma)$. Therefore, we can use the standard interpolation operator on triangular meshes for quadratic trial functions to get some $\widetilde{v}_g$. Due to this choice and since $h_K = 1$, it is

$$\|v - \widetilde{v}_g\|_{H^1(K)} \leq c_1\, |v|_{H^2(K)},$$

see [3], where the constant c_1 only depends on C and, therefore, on the maximal aspect ratio σ. The reverse triangular inequality yields

$$\|\widetilde{v}_g\|_{H^1(K)} \leq c_1\, |v|_{H^2(K)} + \|v\|_{H^1(K)} \leq \max\{1, c_1\}\, \|v\|_{H^2(K)}$$

The function $\widetilde{v}_0$ fulfils

$$\text{Find } \widetilde{v}_0 \in H_0^1(K): \quad \int_K \nabla\widetilde{v}_0\cdot\nabla w = (\alpha_K, w)_{L_2(K)} - \int_K \nabla\widetilde{v}_g\cdot\nabla w, \quad \forall w \in H_0^1(K).$$

In [7], the Poincaré inequality is stated as

$$\|\widetilde{v}_0\|_{L_2(K)} \leq \left(\frac{1}{\pi}|K|\right)^{1/2} |\widetilde{v}_0|_{H^1(K)}.$$

According to this inequality and since $|K| \leq h_K^2 = 1$, it is

$$\|\widetilde{v}_0\|_{H_1(K)}^2 = \|\widetilde{v}_0\|_{L_2(K)}^2 + |\widetilde{v}_0|_{H_1(K)}^2 \leq \left(1 + \pi^{-1}\right) |\widetilde{v}_0|_{H_1(K)}^2.$$

Due to the variational formulation for $\widetilde{v}_0$, we find with the help of Cauchy-Schwarz inequality as well as Poincaré inequality that

$$\begin{aligned} |\widetilde{v}_0|_{H^1(K)}^2 &= \left| (\alpha_K, \widetilde{v}_0)_{L_2(K)} - \int_K \nabla\widetilde{v}_g\cdot\nabla\widetilde{v}_0 \right| \\ &\leq |\alpha_K||K|^{1/2}\|\widetilde{v}_0\|_{L_2(K)} + |\widetilde{v}_g|_{H^1(K)}|\widetilde{v}_0|_{H^1(K)} \\ &\leq \pi^{-1/2}|\alpha_K||K||\widetilde{v}_0|_{H^1(K)} + |\widetilde{v}_g|_{H^1(K)}|\widetilde{v}_0|_{H^1(K)} \end{aligned}$$

which yields

$$|\widetilde{v}_0|_{H^1(K)} \leq \pi^{-1/2}|\alpha_K||K| + |\widetilde{v}_g|_{H^1(K)}. \tag{5}$$

In the next step, the term $|\alpha_K|$ is estimated. We need the Sobolev embedding theorem which states

$$\|w\|_{C^0(\overline{K})} \leq C_S \|w\|_{H^2(K)} \quad \text{for } w \in H^2(K).$$

The constant C_S is independent of the choice of $K \in \mathcal{K}_h$ since the boundaries of all elements in the mesh $\mathcal{K}_h$ are uniformly Lipschitz. Therefore, we have

$$\begin{aligned} |\alpha_K| &\leq \frac{1}{|\psi_K(z_K)|}\left(|v(z_K)| + \sum_{z\in\mathcal{N}_h : z\in K} |\alpha_{\psi_z}|\psi_z(z_K) + \sum_{E\in\mathcal{E}_h : E\subset\partial K} |\alpha_{\psi_E}|\psi_E(z_K)\right) \\ &\leq \frac{1}{|\psi_K(z_K)|}\left(1 + \sum_{z\in\mathcal{N}_h : z\in K} \psi_z(z_K) + \sum_{E\in\mathcal{E}_h : E\subset\partial K} 2\psi_E(z_K)\right)\|v\|_{C^0(\overline{K})}. \end{aligned}$$

The whole term in big brackets is harmonic as a function of z_K in K. It reaches its maximum on the boundary ∂K because of the maximum principle and is therefore smaller or equal four. We get

$$|\alpha_K| \leq \frac{4C_S}{|\psi_K(z_K)|}\|v\|_{H^2(K)}$$

and have to estimate $\psi_K(z_K)$. Let

$$p(x) = \frac{1}{4}\left(\rho_K^2 - |x - z_K|^2\right) \quad \text{for } x \in K$$

and let $B_{\rho_K}(z_K) \subset K$ be the circle with radius ρ_K and center z_K. Because of the weak minimum principle, we know that $\psi_K \geq 0$ in K. It is

$$\begin{aligned} \Delta\left(\psi_K - p\right) = 0 \quad &\text{in } B_{\rho_K}(z_K) \text{ and} \\ \psi_K - p \geq 0 \quad &\text{on } \partial B_{\rho_K}(z_K). \end{aligned}$$

The minimum principle yields $\psi_K(x) \geq p(x)$ for $x \in B_{\rho_K}(z_K)$ and especially $\psi_K(z_K) \geq \rho_K^2/4$. Finally, we obtain

$$|\alpha_K| \leq \frac{8C_S}{\rho_K^2}\|v\|_{H^2(K)}$$

which gives together with (5)

$$\begin{aligned} |\widetilde{v}_0|_{H^1(K)} &\leq 8\pi^{-1/2}C_S\,\frac{|K|}{\rho_K^2}\,\|v\|_{H^2(K)} + |\widetilde{v}_g|_{H^1(K)} \\ &\leq c_2\,\|v\|_{H^2(K)} + \|\widetilde{v}_g\|_{H^1(K)}. \end{aligned}$$

The constant c_2 only depends on σ since $|K| \leq h_K^2$ and $h_K^2/\rho_K^2 \leq \sigma^2$. The final step in the proof is to combine all estimates.

$$\begin{aligned}
\|\mathfrak{I}^{(3)}v\|_{H^1(K)} &\leq \|\widetilde{v}_0\|_{H^1(K)} + \|\widetilde{v}_g\|_{H^1(K)} \\
&\leq \sqrt{1+\pi^{-1/2}}\,|\widetilde{v}_0|_{H^1(K)} + \|\widetilde{v}_g\|_{H^1(K)} \\
&\leq \sqrt{1+\pi^{-1/2}}\,\left(c_2\,\|v\|_{H^2(K)} + \|\widetilde{v}_g\|_{H^1(K)}\right) + \|\widetilde{v}_g\|_{H^1(K)} \\
&\leq c_2\sqrt{1+\pi^{-1/2}}\,\|v\|_{H^2(K)} + \max\{1,c_1\}\left(1+\sqrt{1+\pi^{-1/2}}\right)\|v\|_{H^2(K)} \\
&= c\,\|v\|_{H^2(K)}.
\end{aligned}$$

The first inequality can be proven in the same way. Here, one uses a lower order interpolation on the triangulation and α_K vanishes in the auxiliary problem (4) which simplifies the proof. □

The polynomial approximations of functions in Sobolev-spaces and their properties are important. Especially, the following Lemma is of interest.

Lemma 3. *Let $\Omega \subset \mathbb{R}^2$ be a bounded convex domain with diameter h_Ω and let $v \in H^{k+1}(\Omega)$ for $k \in \mathbb{N}$. Then there exist a polynomial $p \in \mathcal{P}^k(\Omega)$ and a constant $C = C(j,k)$ with*

$$|v-p|_{H^j(\Omega)} \leq C\,h_\Omega^{k+1-j}\,|v|_{H^{k+1}(\Omega)} \quad \text{for } j = 0,1,\ldots,k+1.$$

For a proof see [5, 17]. A simple consequence of this lemma is the estimate

$$\|v-p\|_{H^2(K)} \leq C\,|v|_{H^2(K)}$$

for a function $v \in H^2(K)$ with corresponding $p \in \mathcal{P}^1(K)$ and the estimate

$$\|v-p\|_{H^2(K)} \leq Ch_K|v|_{H^3(K)} \tag{6}$$

for a function $v \in H^3(K)$ with corresponding $p \in \mathcal{P}^2(K)$. The constant C is independent of the element K.
With the help of the previous considerations, we can state the main results for the interpolation error.

Theorem 1. *For a regular mesh $\mathcal{K}_h$ of a bounded polygonal domain $\Omega \subset \mathbb{R}^2$, the interpolation operators $\mathfrak{I}^{(i)} : H^2(\Omega) \to \operatorname{span}\Psi^{(i)}$, $i = 1,3$ fulfil*

$$\|v-\mathfrak{I}^{(1)}v\|_{H^1(\Omega)} \leq c\,h\,|v|_{H^2(\Omega)} \quad \text{for } v \in H^2(\Omega)$$

and

$$\|v-\mathfrak{I}^{(3)}v\|_{H^1(\Omega)} \leq c\,h^2\,|v|_{H^3(\Omega)} \quad \text{for } v \in H^3(\Omega),$$

where $h = \max\{h_K : K \in \mathcal{K}_h\}$ and the constant c only depends on the maximal aspect ratio σ of the mesh.

Proof. The first inequality has already been proven in [8] and thus we restrict ourself to the second estimate. Lets start to examine the error over one element $K \in \mathcal{K}_h$. We have to scale this element in such a way that its diameter becomes one. The scaled element is denoted by $\widehat{K}$ and we define the affine map

$$\widehat{x} \in \widehat{K} \mapsto x = F(\widehat{x}) = B\widehat{x}$$

with the matrix $B = h_K I$. We have $F : \widehat{K} \to K$ and $\det B = h_K^2$, $\|B\|_2 = h_K$ as well as $\|B^{-1}\|_2 = h_K^{-1}$. Let $v \in H^k(K)$, then it is $\widehat{v} = v \circ F \in H^k(\widehat{K})$ with

$$|\widehat{v}|_{H^k(\widehat{K})} \leq c\|B\|_2^k |\det B|^{-1/2} |v|_{H^k(K)}$$

and

$$|v|_{H^k(K)} \leq c\|B^{-1}\|_2^k |\det B|^{1/2} |\widehat{v}|_{H^k(\widehat{K})}$$

where the constant c only depends on $k \in \mathbb{N}_0$, see [3].
Let $\widehat{\mathfrak{I}}^{(3)}$ be the interpolation operator with respect to $\widehat{K}$. Due to the pointwise interpolation, it does not matter if v is first transformed into $\widehat{v}$ and then interpolated or if v is first interpolated $\mathfrak{I}^{(3)}v$ and then transformed. This means

$$\widehat{\mathfrak{I}}^{(3)}\widehat{v} = \widehat{\mathfrak{I}^{(3)}v}.$$

Consequently, we obtain

$$\begin{aligned} \|v - \mathfrak{I}^{(3)}v\|_{H^1(K)}^2 &= \|v - \mathfrak{I}^{(3)}v\|_{L_2(K)}^2 + |v - \mathfrak{I}^{(3)}v|_{H^1(K)}^2 \\ &\leq ch_K^2 \|\widehat{v} - \widehat{\mathfrak{I}}^{(3)}\widehat{v}\|_{L_2(\widehat{K})}^2 + c\,|\widehat{v} - \widehat{\mathfrak{I}}^{(3)}\widehat{v}|_{H^1(\widehat{K})}^2 \\ &\leq c\,\|\widehat{v} - \widehat{\mathfrak{I}}^{(3)}\widehat{v}\|_{H^1(\widehat{K})}^2 \end{aligned}$$

since $h_K \leq 1$. Let $\widehat{p} \in \mathcal{P}^2(\widehat{K})$ be the polynomial of Lemma 3 which closely approximates $\widehat{v}$. Applying Lemma 1 and Lemma 2, we obtain

$$\begin{aligned} \|\widehat{v} - \widehat{\mathfrak{I}}^{(3)}\widehat{v}\|_{H^1(\widehat{K})} &\leq \|\widehat{v} - \widehat{p}\|_{H^1(\widehat{K})} + \|\widehat{\mathfrak{I}}^{(3)}(\widehat{v} - \widehat{p})\|_{H^1(\widehat{K})} \\ &\leq (1+c)\,\|\widehat{v} - \widehat{p}\|_{H^2(\widehat{K})} \\ &\leq (1+c)C\,|\widehat{v}|_{H^3(\widehat{K})}, \end{aligned}$$

where we also have used (6). Comparing the last two estimates and transforming back to the element K yields

$$\|v - \mathfrak{I}^{(3)}v\|_{H^1(K)}^2 \leq ch_K^4\,|v|_{H^3(K)}^2.$$

In the last step of the proof, we have to sum up this inequality over all elements of the mesh and apply the square root to it. This gives

$$\|v - \mathfrak{I}^{(3)}v\|_{H^1(\Omega)} \leq c\left(\sum_{K\in\mathcal{K}_h} h_K^4\,|v|_{H^3(K)}^2\right)^{1/2} \leq c\,h^2\,|v|_{H^3(K)}$$

and finishes the proof. □

As mentioned in the beginning of this section, error estimates for interpolation operators carry over to approximation errors of the finite element method. Céa's-Lemma together with the last Theorem yield

$$\|u - u_h\|_{H^1(\Omega)} \leq c\, h\, |u|_{H^2(\Omega)} \quad \text{for } u \in H^2(\Omega)$$

in case of the lower order method, i.e. $V_h = \operatorname{span}\{\Psi^{(1)} \setminus \Psi_D\}$, and

$$\|u - u_h\|_{H^1(\Omega)} \leq c\, h^2\, |u|_{H^3(\Omega)} \quad \text{for } u \in H^3(\Omega)$$

in case of higher order trial functions, i.e. $V_h = \operatorname{span}\{\Psi^{(3)} \setminus \Psi_D\}$.
Finally, we stat an interpolation error estimate in the L_2-Norm.

Lemma 4. *For a regular mesh $\mathcal{K}_h$ of a bounded polygonal domain $\Omega \subset \mathbb{R}^2$, the interpolation operator $\mathfrak{I}^{(1)} : H^2(\Omega) \to \operatorname{span} \Psi^{(1)}$ fulfils*

$$\|v - \mathfrak{I}^{(1)} v\|_{L_2(\Omega)} \leq c\, h^2\, |v|_{H^2(\Omega)} \quad \textit{for } v \in H^2(\Omega)$$

where $h = \max\{h_K : K \in \mathcal{K}_h\}$ and the constant c only depends on the maximal aspect ratio σ of the mesh.

Proof. Using the same ideas as in the proof of Theorem 1 yields for $v \in H^2(\Omega)$

$$\begin{aligned} \|v - \mathfrak{I}^{(1)} v\|_{L_2(K)} &\leq ch_K \|\widehat{v} - \widehat{\mathfrak{I}}^{(1)} \widehat{v}\|_{L_2(\widehat{K})} \leq ch_K \|\widehat{v} - \widehat{\mathfrak{I}}^{(1)} \widehat{v}\|_{H^1(\widehat{K})} \\ &\leq ch_K |\widehat{v}|_{H^2(\widehat{K})} \leq ch_K^2 |v|_{H^2(K)}. \end{aligned}$$

Summing up the square of these terms finishes the proof. □

5 Diffusion coefficient

All examples in Section 2 and 3 have been Poisson problems with material coefficient $a(\cdot) \equiv 1$. Since the numerical scheme presented in [4] can handle piecewise constant coefficients there is no error with respect to the coefficient. In the general case, a piecewise constant approximation $a^h(\cdot)$ of $a(\cdot)$ is needed.
In Example 5, we can recognize that this coarse approximation of the material coefficient seems to be enough in case of the lower order method, whereas the convergence of the higher order method slows down due to this approximation error.

Example 5. The function $u(x) = |x - x^*|$, $x \in \mathbb{R}^2$ with $x^* = (-0.1, 0.2)^\top$ fulfils

$$\begin{aligned} -\operatorname{div}\left(\frac{1}{|x - x^*|} \nabla u\right) &= 0 \quad \text{in } \Omega = [0,1]^2, \\ u &= g_D \quad \text{on } \Gamma \end{aligned} \tag{7}$$

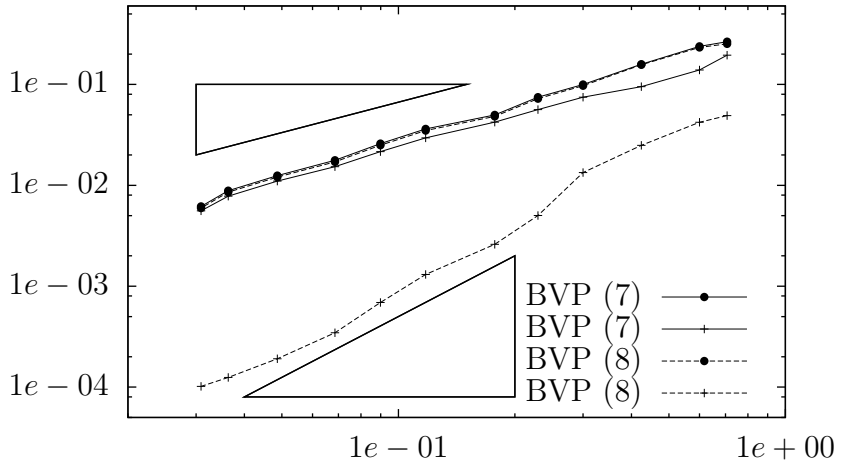

Figure 6: Absolute error with respect to h in the H^1-norm for problem (7) and (8) in Example 5 with $\Psi = \Psi^{(1)} \setminus \Psi_D$ ($\bullet$) and $\Psi = \Psi^{(3)} \setminus \Psi_D$ ($+$), respectively, and triangles with slope one and two

as well as

$$\begin{aligned} -\Delta u &= f \quad \text{in } \Omega = [0,1]^2, \\ u &= g_D \quad \text{on } \Gamma \end{aligned} \tag{8}$$

with $g_D = \gamma_0 u$ and $f(x) = -|x - x^*|^{-1}$. The convergence can be seen in Figure 6 for the finite element method on a sequence of uniform refined meshes.

To analyse the impact of the approximation error of the material coefficient, the first Strang-Lemma [15] is used. Replacing the exact material coefficient in the bilinear form $a_\Omega(\cdot,\cdot)$ by an approximated one can be seen as an approximation $a_\Omega^h(\cdot,\cdot)$ of the bilinear form. We restrict ourself to approximations $a^h(\cdot)$ of the material coefficient which fulfil

$$0 < a_{\min} \leq a^h(x) \leq a_{\max} \quad \text{for } x \in \Omega \text{ and } h > 0.$$

Therefore, the bilinear form $a_\Omega^h(\cdot,\cdot)$ is uniformly coercive as well as bounded on V_h for $h > 0$, and the variational formulation has a unique solution. The following formulation of the Strang-Lemma can be found in [3].

Lemma 5. *Consider a family of discrete problems whose associated approximate bilinear forms $a_\Omega^h : V_h \times V_h \to \mathbb{R}$ are uniformly V_h-elliptic. Then there exists a constant C independent of the space V_h such that*

$$\|u - u_h\|_{H^1(\Omega)} \leq C \inf_{v_h \in V_h} \left\{ \|u - v_h\|_{H^1(\Omega)} + \sup_{w_h \in V_h} \frac{|a_\Omega(v_h, w_h) - a_\Omega^h(v_h, w_h)|}{\|w_h\|_{H^1(\Omega)}} \right\}.$$

Obviously, the approximation error in the finite element method is estimated by a constant times two terms. One which gives the best approximation error and one which measures the error coming from the inexact bilinear form. Choosing $v_h = \mathfrak{I}^{(3)}u$ in the lemma yields

$$\|u - u_h\|_{H^1(\Omega)} \leq C\|u - \mathfrak{I}^{(3)}u\|_{H^1(\Omega)} + \sup_{w_h \in V_h} \frac{|a_\Omega(\mathfrak{I}^{(3)}u, w_h) - a_\Omega^h(\mathfrak{I}^{(3)}u, w_h)|}{\|w_h\|_{H^1(\Omega)}}.$$

In Figure 7, we can see that for Example 5 the interpolation error converges with second order. This coincides with the theory of Section 4 which gives us quadratic convergence for the interpolation of a function $u \in H^3(\Omega)$ in the Sobolev-norm. Hence, the approximation quality of the bilinear form is responsible for the reduced rate of convergence for the finite element method. To improve the approximation of the bilinear form, we propose to use a globally continuous approximation $a^h = \mathfrak{I}^{(1)}a$. Due to this choice the numerical realisation described in [4] does not work any more. This problem is discussed in the next section.
The following example shows the optimal convergence for a problem with varying material properties.

Example 6. We solve again the first problem mentioned in Example 5 and use the approximation $a^h = \mathfrak{I}^{(1)}a$ for the material coefficient instead of a piecewise constant one. In Figure 7, we can recognize the improved rate of convergence due to the better approximation of the material coefficient and the convergence of the interpolation error $\|u - \mathfrak{I}^{(3)}u\|_{H^1(\Omega)}$.

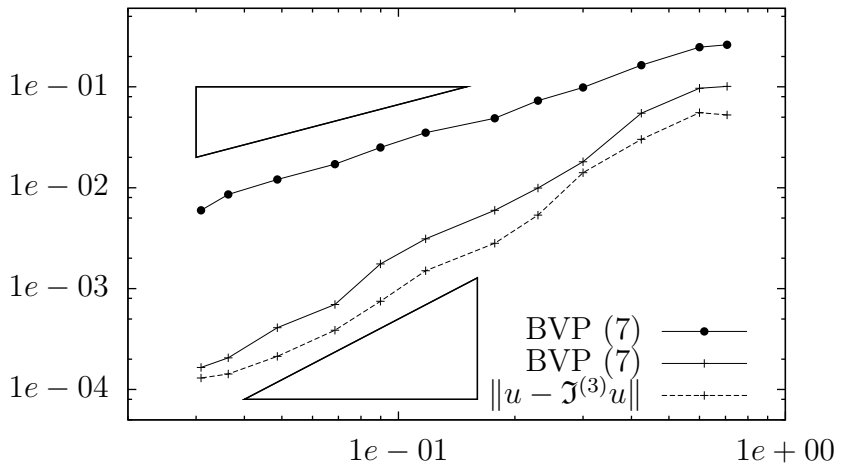

Figure 7: Absolute error with respect to h in the H^1-norm for improved approximation of $a_\Omega(\cdot,\cdot)$ in Example 6 with $\Psi = \Psi^{(1)} \setminus \Psi_D$ ($\bullet$) and $\Psi = \Psi^{(3)} \setminus \Psi_D$ ($+$), respectively, and interpolation error $\|u - \mathfrak{I}^{(3)}u\|_{H^1(\Omega)}$ as well as triangles with slope one and two

6 Numerical realisation

In the previous sections, we have seen the Galerkin-formulation and the corresponding approximations of solutions of different boundary value problems. Nevertheless, the difficulty to compile the stiffness matrix has not been addressed till now.
For the approximation of the extended boundary data u_D, we use

$$u_{Dh} = \sum_{\psi \in \Psi_D} \beta_\psi \psi \quad \text{with} \quad \Psi_D = \{\psi_z, \psi_E : z \in \mathcal{N}_{h,D}, E \in \mathcal{E}_{h,D}\},$$

where the coefficients β_ψ are obtained by interpolation of g_D. The ansatz (1) together with the Galerkin-formulation yield the following system of liner equations

$$\sum_{\psi \in \Psi} \beta_\psi \, a_\Omega(\psi, \phi) = (f, \phi) + (g_N, \phi)_{\Gamma_N} - \sum_{\psi \in \Psi_D} \beta_\psi \, a_\Omega(\psi, \phi) \quad \text{for } \phi \in \Psi.$$

In the approximation of u_{0h} and u_{Dh}, we use the same symbol β_ψ for the coefficients but there should be no confusion since $\Psi \cap \Psi_D = \varnothing$. We can see that the main topic is to evaluate the bilinear form $a_\Omega(\cdot, \cdot)$ applied to trial functions in the set up of the system. The boundary integral $(g_N, \phi)_{\Gamma_N}$ can be computed quite easy since the function ϕ is a piecewise quadratic polynomial over Γ_N. To handle (f, ϕ), we can split the volume integral over Ω into integrals over elements and use numerical integration over each polygonal region. For this quadrature, it is possible to split the polygon even further into triangles or to use appropriate quadrature rules for polygonal elements, see [12].
In the following, we need the usual trace operator $\gamma_0^K : H^1(K) \to H^{1/2}(\partial K)$ which is defined in [1], for example. Let $v \in H^1(K)$ with Δv in the dual of $H^1(K)$. Due to Green's first identity [11], there exists a unique function $\gamma_1^K v \in H^{-1/2}(\partial K)$ such that

$$\int_K \nabla v(y) \cdot \nabla w(y) \, dy = \int_{\partial K} \gamma_1^K v(y) \gamma_0^K w(y) \, ds_y - \int_K w(y) \Delta v(y) \, dy$$

for $w \in H^1(K)$. We call $\gamma_1^K v$ the conormal derivative of v. If v is smooth, e.g. $v \in H^2(K)$ like the trial functions, we have

$$(\gamma_1^K v)(x) = n_K(x) \cdot (\gamma_0^K \nabla v)(x) \quad \text{for } x \in \partial K,$$

where $n_K(x)$ denotes the outer normal vector of the element K at x. The trace and the conormal derivative are also called Dirichlet and Neumann trace for the Laplace equation and both γ_0^K and γ_1^K are linear operators. In the case of a trial function $\psi \in \Psi^{(3)}$ it is $\gamma_0^K \psi = \psi$ on ∂K since we have $\psi \in C^2(K) \cap C^0(\overline{K})$.

Therefore, we omit the trace operator γ_0^K in boundary integrals if no confusion occurs.
As proposed in Section 5, the material coefficient is approximated by the interpolant $\mathfrak{I}^{(1)}a$, that means

$$a^h(x) = \sum_{\lambda\in\Psi^{(1)}} \alpha_\lambda \lambda(x) \quad \text{with} \quad \alpha_{\lambda_z} = a(z),\ z \in \mathcal{N}_h.$$

Remember $\Delta\lambda = 0$ in all $K \in \mathcal{K}_h$ and let $\psi, \phi \in \Psi$, then

$$\nabla\psi \cdot \nabla\phi = \frac{1}{2}\big(\Delta(\psi\phi) - \psi\Delta\phi - \phi\Delta\psi\big)$$

together with Green's second identity yield

$$\begin{aligned} a_\Omega(\psi,\phi) \approx a^h_\Omega(\psi,\phi) &= \int_\Omega a^h \nabla\psi\cdot\nabla\phi = \sum_{K\in\mathcal{K}_h,\lambda\in\Psi^{(1)}} \alpha_\lambda \int_K \lambda\nabla\psi\cdot\nabla\phi \\ &= \sum_{K\in\mathcal{K}_h,\lambda\in\Psi^{(1)}} \frac{\alpha_\lambda}{2}\bigg\{\int_K (\lambda\Delta(\psi\phi) - \psi\phi\Delta\lambda) - \int_K \lambda\psi\Delta\phi - \int_K \lambda\phi\Delta\psi\bigg\} \\ &= \sum_{K\in\mathcal{K}_h,\lambda\in\Psi^{(1)}} \frac{\alpha_\lambda}{2}\bigg\{\int_{\partial K} \big(\lambda\phi\,\gamma_1^K\psi + \lambda\psi\,\gamma_1^K\phi - \psi\phi\,\gamma_1^K\lambda\big) - \int_K (\lambda\psi\Delta\phi + \lambda\phi\Delta\psi)\bigg\}. \end{aligned}$$

At first glance, this representation for the bilinear form looks more complicated than the standard one. But it turns out that it has some advantages. Depending on the sort of trial and test functions many terms vanish. For example, let $\psi, \phi \in \Psi^{(2)}$ then the volume integral is zero since ψ and ϕ are harmonic. In particular, the only case when the volume integral does not vanish is that ψ or ϕ is an element bubble function and the Laplacian of this function is minus one. Hence, we have to evaluate integrals like

$$\int_K \lambda\psi \quad \text{with } \lambda \in \Psi^{(1)} \text{ and } \psi \in \Psi^{(3)} \text{ for } K \in \mathcal{K}_h.$$

In the implementation, this integration is done with the help of numerical quadrature using the representation formula for λ and ψ, see below.
The boundary integral contains three terms which are similar to each other. Obviously, it is sufficient to study

$$\int_{\partial K} \lambda\phi\,\gamma_1^K\psi \quad \text{for } \lambda,\phi,\psi \in \Psi^{(3)}. \tag{9}$$

Here, the conormal derivative as well as the traces of the trial and test functions are involved. In the following the boundary integral formulation is used to handle

this kind of integrals and to find a representation formula to evaluate the trial functions in the interior of elements.
Let $K \in \mathcal{K}_h$. First, we consider $\psi \in \Psi^{(2)}$ that means ψ fulfils the boundary value problem

$$\begin{aligned} -\Delta\psi &= 0 \quad \text{in } K, \\ \psi &= g \quad \text{on } \partial K \end{aligned} \tag{10}$$

with some piecewise quadratic function g on ∂K. The solution ψ of the Laplace problem can be expressed in terms of boundary integrals, see e.g. [11]. According to that, the representation formula reads

$$\psi(x) = \int_{\partial K} U^*(x,y)\gamma_1^K\psi(y)\,ds_y - \int_{\partial K} \gamma_{1,y}^K U^*(x,y)\gamma_0^K\psi(y)\,ds_y \quad \text{for } x \in K,$$

where U^* is the fundamental solution of the Laplacian with

$$U^*(x,y) = -\frac{1}{2\pi}\ln|x-y| \quad \text{for } x,y \in \mathbb{R}^2.$$

The Dirichlet trace $\gamma_0^K\psi = g$ is given and one has to find an expression for $\gamma_1^K\psi$. If we have found this it is possible to evaluate ψ everywhere in K. Applying the trace operator and the conormal derivative operator to the representation formula yields the system of equations

$$\begin{pmatrix} \gamma_0^K\psi \\ \gamma_1^K\psi \end{pmatrix} = \begin{pmatrix} \frac{1}{2}\mathbf{I} - \mathbf{K}_K & \mathbf{V}_K \\ \mathbf{D}_K & \frac{1}{2}\mathbf{I} + \mathbf{K}_K' \end{pmatrix} \begin{pmatrix} \gamma_0^K\psi \\ \gamma_1^K\psi \end{pmatrix}. \tag{11}$$

The system contains the standard boundary integral operators which are well studied, see e.g. [11, 14]. For $x \in \partial K$, we have the single-layer potential operator

$$(\mathbf{V}_K\zeta)(x) = \gamma_0^K \int_{\partial K} U^*(x,y)\zeta(y)\,ds_y \quad \text{for } \zeta \in H^{-1/2}(\partial K),$$

the double-layer potential operator

$$(\mathbf{K}_K\xi)(x) = \lim_{\varepsilon\to 0} \int_{y\in\partial K:|y-x|\geq\varepsilon} \gamma_{1,y}^K U^*(x,y)\xi(y)\,ds_y \quad \text{for } \xi \in H^{1/2}(\partial K),$$

and the adjoint double-layer potential

$$(\mathbf{K}_K'\zeta)(x) = \lim_{\varepsilon\to 0} \int_{y\in\partial K:|y-x|\geq\varepsilon} \gamma_{1,x}^K U^*(x,y)\zeta(y)\,ds_y \quad \text{for } \zeta \in H^{-1/2}(\partial K),$$

as well as the hypersingular integral operator

$$(\mathbf{D}_K\xi)(x) = -\gamma_1^K \int_{\partial K} \gamma_{1,y}^K U^*(x,y)\xi(y)\,ds_y \quad \text{for } \xi \in H^{1/2}(\partial K).$$

Since the diameter of K is smaller than one, the single-layer potential operator is invertible and the first equation of the system (11) yields a connection between the Dirichlet and the Neumann trace

$$\gamma_1^K \psi = \mathbf{S}_K \gamma_0^K \psi \quad \text{with} \quad \mathbf{S}_K = \mathbf{V}_K^{-1} \left(\tfrac{1}{2}\mathbf{I} + \mathbf{K}_K \right).$$

The operator $\mathbf{S}_K : H^{1/2}(\partial K) \to H^{-1/2}(\partial K)$ is called Steklov-Poincaré operator. Using the second equation of the system (11) we can find the symmetric representation

$$\mathbf{S}_K = \mathbf{D}_K + \left(\tfrac{1}{2}\mathbf{I} + \mathbf{K}_K' \right) \mathbf{V}_K^{-1} \left(\tfrac{1}{2}\mathbf{I} + \mathbf{K}_K \right).$$

To realise the Dirichlet to Neumann map in the numerics, the Steklov-Poincaré operator has to be discretize. For this reason, we introduce the space of piecewise quadratic and globally continuous functions on ∂K to approximate $H^{1/2}(\partial K)$. More precise, we use the basis

$$\Phi_D = \{ \gamma_0^K \psi_z, \gamma_0^K \psi_E : z \in \partial K, E \subset \partial K \}$$

of that space. Additionally, let

$$\Phi_N = \{ \tau_E^0, \tau_E^1 : E \subset \partial K \}$$

where $\tau_E^0, \tau_E^1 : \partial K \to \mathbb{R}$ with

$$\tau_E^0 = \begin{cases} 1, & \text{on } E \\ 0, & \text{else} \end{cases} \qquad \text{and} \qquad \tau_E^1 = \begin{cases} 1, & \text{at } z_e \\ \text{linear}, & \text{on } E \\ 0, & \text{else} \end{cases}$$

for $E = \overline{z_b z_e}$. The set Φ_N forms a basis of the space of piecewise linear functions which is used to approximate $H^{-1/2}(\partial K)$.
We come back to the boundary value problem (10) for ψ. The Dirichlet data $\gamma_0^K \psi = g \in \operatorname{span} \Phi_D$ is given and the Neumann data $\gamma_1^K \psi$ is approximated by $t \in \operatorname{span} \Phi_N$ using the Galerkin-formulation

$$\text{Find } t \in \operatorname{span} \Phi_N : \quad \left(\mathbf{V}_K t, \vartheta \right)_{L_2(\partial K)} = \left(\left(\tfrac{1}{2}\mathbf{I} + \mathbf{K}_K \right) g, \vartheta \right)_{L_2(\partial K)} \quad \forall \vartheta \in \Phi_N.$$

Due to the properties of the boundary integral operators, this formulation has a unique solution. The representations

$$t = \sum_{\tau \in \Phi_N} t_\tau \tau \qquad \text{and} \qquad g = \sum_{\varphi \in \Phi_D} g_\varphi \varphi$$

yield the system of linear equations

$$\mathbf{V}_{K,h} \underline{t} = \left(\tfrac{1}{2}\mathbf{M}_{K,h} + \mathbf{K}_{K,h} \right) \underline{g},$$

where the underline refers to the coefficient vector, e.g. $\underline{t} = (t_\tau)_{\tau\in\Phi_N}$. The matrices are defined as

$$\mathbf{V}_{K,h} = \Big((\mathbf{V}_K\tau, \vartheta)_{L_2(\partial K)}\Big)_{\vartheta\in\Phi_N,\tau\in\Phi_N}$$

and

$$\mathbf{M}_{K,h} = \Big((\varphi, \vartheta)_{L_2(\partial K)}\Big)_{\vartheta\in\Phi_N,\varphi\in\Phi_D}, \quad \mathbf{K}_{K,h} = \Big((\mathbf{K}_K\varphi, \vartheta)_{L_2(\partial K)}\Big)_{\vartheta\in\Phi_N,\varphi\in\Phi_D}.$$

Furthermore, we use

$$\widetilde{\mathbf{S}}_K g = \mathbf{D}_K g + \left(\tfrac{1}{2}\mathbf{I} + \mathbf{K}'_K\right) t$$

as approximation of the symmetric representation of the Steklov-Poincaré operator.
Insted of considering the integral (9) directly, we define the set

$$\Phi_{Ex} = \{\gamma_0^K(\psi_{z_b}\psi_{z_e}), \gamma_0^K(\psi_{z_b}\psi_{z_b}), \gamma_0^K(\psi_{z_b}\psi_E), \gamma_0^K(\psi_{z_e}\psi_E), \gamma_0^K(\psi_E\psi_E) : E \subset \partial K\}$$

and choose an arbitrary function $q \in \operatorname{span}\Phi_{Ex}$ with

$$q = \sum_{\chi\in\Phi_{Ex}} q_\chi \chi.$$

It is

$$\begin{aligned}
\int_{\partial K} q\,\gamma_1^K\psi &\approx \int_{\partial K} q\,\widetilde{\mathbf{S}}_K g = \left(q, \mathbf{D}_K g + \left(\tfrac{1}{2}\mathbf{I} + \mathbf{K}'_K\right) t\right)_{L_2(\partial K)} \\
&= (\mathbf{D}_K g, q)_{L_2(\partial K)} + \tfrac{1}{2}(q,t)_{L_2(\partial K)} + (\mathbf{K}_K q, t)_{L_2(\partial K)} \\
&= \underline{q}^\top \mathbf{D}^{Ex}_{K,h}\underline{g} + \underline{q}^\top\left(\tfrac{1}{2}\left(\mathbf{M}^{Ex}_{K,h}\right)^\top + \left(\mathbf{K}^{Ex}_{K,h}\right)^\top\right)\underline{t} \\
&= \underline{q}^\top \mathbf{D}^{Ex}_{K,h}\underline{g} + \underline{q}^\top\left(\tfrac{1}{2}\left(\mathbf{M}^{Ex}_{K,h}\right)^\top + \left(\mathbf{K}^{Ex}_{K,h}\right)^\top\right)\mathbf{V}^{-1}_{K,h}\left(\tfrac{1}{2}\mathbf{M}_{K,h} + \mathbf{K}_{K,h}\right)\underline{g} \\
&= \underline{q}^\top \mathbf{S}^{Ex}_{K,h}\underline{g},
\end{aligned}$$

where

$$\mathbf{S}^{Ex}_{K,h} = \mathbf{D}^{Ex}_{K,h} + \left(\tfrac{1}{2}\left(\mathbf{M}^{Ex}_{K,h}\right)^\top + \left(\mathbf{K}^{Ex}_{K,h}\right)^\top\right)\mathbf{V}^{-1}_{K,h}\left(\tfrac{1}{2}\mathbf{M}_{K,h} + \mathbf{K}_{K,h}\right)$$

with

$$\mathbf{D}^{Ex}_{K,h} = \Big((\mathbf{D}_K\varphi, \chi)_{L_2(\partial K)}\Big)_{\chi\in\Phi_{Ex},\varphi\in\Phi_D}$$

and

$$\mathbf{M}^{Ex}_{K,h} = \Big((\chi,\tau)_{L_2(\partial K)}\Big)_{\tau\in\Phi_N,\chi\in\Phi_{Ex}}, \quad \mathbf{K}^{Ex}_{K,h} = \Big((\mathbf{K}_K\chi,\tau)_{L_2(\partial K)}\Big)_{\tau\in\Phi_N,\chi\in\Phi_{Ex}}.$$

Since $q = \lambda\phi \in \Phi_{Ex}$ for the integral (9) and $g \in \Phi_D$ for $\psi \in \Psi^{(2)}$, the coefficient vectors $\underline{q}$ and $\underline{g}$ contain only zeros and a single one. Therefore, the approximation of integral (9) coincides with an entry of the matrix $\mathbf{S}^{Ex}_{K,h}$.

In the case of $\psi \in \Psi^{(3)} \setminus \Psi^{(2)}$, the trial function fulfils for one $K \in \mathcal{K}_h$ the boundary value problem

$$\begin{aligned} -\Delta\psi &= 1 \quad \text{in } K \\ \psi &= 0 \quad \text{on } \partial K \end{aligned} \tag{12}$$

which can be reduced to the previous situation. Therefore, we write $\psi = \psi_h + \psi_p$ with $\psi_p = -\frac{1}{4}|x - z_K|^2$. Then (12) yields

$$\begin{aligned} -\Delta\psi_h &= 0 \quad \text{in } K \\ \psi_h &= g \quad \text{on } \partial K \end{aligned}$$

with $g = -\gamma_0^K \psi_p \in \operatorname{span} \Phi_D$ which can be treated as prescribed earlier. The integral (9) splits into two parts

$$\int_{\partial K} q\, \gamma_1^K \psi = \int_{\partial K} q\, \gamma_1^K \psi_h + \int_{\partial K} q\, \gamma_1^K \psi_p \approx \underline{q}^\top \mathbf{S}_{K,h}^{Ex} \underline{g} + \int_{\partial K} q\, \gamma_1^K \psi_p.$$

In contrast to the previous case, $\underline{g}$ is now a full vector but $\underline{q}$ still contains a single one. The first term of the approximation turns into a scalar product of $\underline{g}$ and a row of $\mathbf{S}_{K,h}^{Ex}$. Due to the construction of ψ_p, the conormal derivative $\gamma_1^K \psi_p$ is constant on each edge $E \subset \partial K$. This fact can easily be seen using the parametrisation $x(s) = z_b + s(z_e - z_b) \in E = \overline{z_b z_e}$ for $0 \le s \le 1$ in

$$\gamma_1^K \psi_z(x) = -\tfrac{1}{2}(x - z_K) \cdot n_K = -\tfrac{1}{2}(z_b - z_K) \cdot n_K - \tfrac{1}{2} s \underbrace{(z_e - z_b) \cdot n_K}_{=0}$$

The function q is a given polynomial of degree less or equal than four on $E \subset \partial K$. Therefore, the boundary integral in the second term of the approximation can be computed analytically.

The final step in the set up of the finite element matrix is to compute all these boundary integral matrices to construct $\mathbf{S}_{K,h}^{Ex}$. The mass matrices $\mathbf{M}_{K,h}$ and $\mathbf{M}_{K,h}^{Ex}$ can be computed analytically, whereas numerical integration is used to compile the others. In the realisation, we utilise an advanced adaptive integration scheme to compute integrals of the form

$$(\mathbf{V}_K \nu, \mu)_{L_2(\partial K)} \quad \text{and} \quad (\mathbf{K}_K \nu, \mu)_{L_2(\partial K)} \tag{13}$$

for

$$\nu \in \left\{ \tau_E^0, \left(\tau_E^1\right)^j : E \subset \partial K, j = 1, \ldots, 4 \right\} \quad \text{and} \quad \mu \in \left\{ \tau_E^0, \tau_E^1 : E \subset \partial K \right\}.$$

Building linear combinations of these integrals, we can construct the matrices $\mathbf{K}_{K,h}^{Ex}$, $\mathbf{K}_{K,h}$ and $\mathbf{V}_{K,h}$. Even the entries of $\mathbf{D}_{K,h}^{Ex}$ can be written as linear combinations of (13), see [14].

The computation of the local boundary integral matrices is highly parallelizable since matrices from different elements are independent. Furthermore, the elements have only a few edges in practice and therefore all appearing matrices are small.

7 Conclusion

The reviewed BEM-based FEM with implicitly defined trial functions is a conforming method that works on general meshes. It can be applied in a wide range of problems but it is just at the beginning of its development. To the best of our knowledge, we have introduced a new kind of higher order trial functions and we have proven higher order convergence estimates for a conforming finite element method on polygonal meshes. To handle the advanced approximation of the material parameter, we came up with a special treatment in the numerics of local boundary element formulations.

References

[1] R. A. Adams. *Sobolev Spaces*. Academic Press, 1975.

[2] F. Brezzi, K. Lipnikov, and M. Shashkov. Convergence of the mimetic finite difference method for diffusion problems on polyhedral meshes. *SIAM J. Numer. Anal.*, 43(5):1872–1896 (electronic), 2005.

[3] P. G. Ciarlet. *The Finite Element Method for Elliptic Problems*. North-Holland, Amsterdam, 1978.

[4] D. Copeland, U. Langer, and D. Pusch. From the boundary element domain decomposition methods to local Trefftz finite element methods on polyhedral meshes. *Domain Decomposition Methods in Science and Engineering XVIII*, pages 315–322, 2009.

[5] S. Dekel and D. Leviatan. The Bramble-Hilbert lemma for convex domains. *SIAM journal on mathematical analysis*, 35(5):1203–1212, 2004.

[6] V. Dolejší, M. Feistauer, and V. Sobotíková. Analysis of the discontinuous Galerkin method for nonlinear convection-diffusion problems. *Comput. Methods Appl. Mech. Engrg.*, 194(25-26):2709–2733, 2005.

[7] D. Gilbarg and N. S. Trudinger. *Elliptic partial differential equations of second order*, volume 224. Springer Verlag, 2001.

[8] A. Gillette, A. Rand, and C. Bajaj. Error estimates for generalized barycentric interpolation. *Advances in Computational Mathematics*, pages 1–23, 2011. 10.1007/s10444-011-9218-z.

[9] C. Hofreither, U. Langer, and C. Pechstein. Analysis of a non-standard finite element method based on boundary integral operators. *Electronic Transactions on Numerical Analysis (ETNA)*, 37:413–436, 2010.

[10] S. Martin, P. Kaufmann, M. Botsch, M. Wicke, and M. Gross. Polyhedral finite elements using harmonic basis functions. *Computer Graphics Forum*, 27(5):1521–1529, 2008.

[11] W. C. H. McLean. *Strongly elliptic systems and boundary integral equations*. Cambridge Univ Pr, 2000.

[12] S. E. Mousavi and N. Sukumar. Numerical integration of polynomials and discontinuous functions on irregular convex polygons and polyhedrons. *Computational Mechanics*, 47:535–554, 2011. 10.1007/s00466-010-0562-5.

[13] A. Rand, A. Gillette, and C. Bajaj. Quadratic serendipity finite elements on polygons using generalized barycentric coordinates. 2011. arXiv/1109.3259.

[14] O. Steinbach. *Numerical approximation methods for elliptic boundary value problems: finite and boundary elements*. Springer, 2007.

[15] G. Strang. Variational crimes in the finite element method. In *The mathematical foundations of the finite element method with applications to partial differential equations (Proc. Sympos., Univ. Maryland, Baltimore, Md., 1972)*, pages 689–710. Academic Press, New York, 1972.

[16] A. Tabarraei and N. Sukumar. Application of polygonal finite elements in linear elasticity. *International Journal of Computational Methods*, 3(4):503–520, 2006.

[17] R. Verfürth. A note on polynomial approximation in Sobolev spaces. *Mathematical Modelling and Numerical Analysis*, 33(4):715–719, 1999.

[18] E. L. Wachspress. *A Rational Finite Element Basis*. Academic Press, 1975.

[19] S. Weißer. Residual error estimate for BEM-based FEM on polygonal meshes. *Numerische Mathematik*, 118:765–788, 2011. 10.1007/s00211-011-0371-6.